

# A Pragmatic Approach for Estimating Residual Life of Micro cracked 17.5MW Turbine-Generator Shafts of Hydropower Plants Through Reassessment of NDT and Fracture Mechanics- A Case Study

**Kumar R K**

Central Power Research Institute, Bangalore-560080

[rkkumar@cpri.in](mailto:rkkumar@cpri.in)

## Abstract

*The present study emphasizes the Residual Life Assessment of a vertical Turbine and Generator rotor shaft of an uprated 17.5 MW hydro plant by Ultrasonic B-scan imaging, followed by the assessment of the remaining life through fatigue crack growth rate studies. The complete turbine shaft geometry was scanned, and the accessible regions of the generator shaft were also analyzed using UT-Bscan. The size and depth of the defect data were obtained. Finite element analysis was carried out to evaluate stresses experienced in the shaft at different locations using the commercial code Ansys Mechanical®. The residual life of the rotor shaft was calculated based on the fracture mechanics principle using the code Ansys and FRANC3DTM, considering the crack close to the shaft's OD surface. For the precise estimation of the residual life of the shaft, the optimized crack growth parameters linked to the expended service hours after the previous inspection were adopted.*

**Keywords:** Hydro turbine generator, damage tolerance, crack growth rate, stress analysis

## 1.0 INTRODUCTION

The refurbishment and uprating of hydro plants in India is being pursued in Indian hydro plants that have completed more than 40 years of service, and many case histories in this regard have been reported [1], [2]. During the Renovation & Modernization programs, the design in terms of insulation grade rotor pole geometry, modified runner, etc., is primarily considered. However, the shaft components are retained, considering the high factor of safety in the original design. Moreover, the replacement of rotor shafts was a challenging exercise since the diameter and length of the shafts are very high, which poses challenges to their manufacturing cycle. The shafts of hydro turbines and generators experience fluctuating loads due to water flow variations, load changes, and rotational forces. This cyclic stress leads to fatigue crack initiation in the regions of stress concentrations, such as the radius at the diametral changes, inclusion, and other crack-like defects that lead

to the shaft's failure in service. Fatigue damage is the primary cause of the failure of hydro turbine shafts [3]. The problems become aggressive under frequent start-stops and load rejection cycles, experienced in many hydro plants. Given the criticality of loading and the high magnitude of torsional stresses during service, they are primarily designed with hollow sections with high safety factors. As these rotors are manufactured through casting and forging routes, they are invariably considered to have process-induced defects like slag, blow holes, etc. [4], [5]. The primary causes of the failure of the hydro turbine and generator shafts are fatigue, misalignment, corrosion, and torsional overloads. The cyclic operation of the units linked to the integration of fossil and renewable-based power generation invariably causes the rotating components to fatigue. Several major failures have led to plant shutdowns, but regular condition monitoring of the shaft components would ensure the safe and reliable operation of the system. The rotor shafts of hydro plants installed

during the late '60s have been designed with a high safety factor since there was no ultrasonic test equipment. Thus, the evaluation of the safe life of the critical turbine-generator shafts of hydro plants is critical based on the criticality of the defects unattended during the regular inspection cycles. Regular condition monitoring of these rotors is being practised, particularly for older plants with uprated capacities.

In the conventional ultrasonic test method, defects such as cracks, inclusions, discontinuity, etc., can be done with depth information inside the component. However, evaluation of the defect orientation is not possible. The application of advanced ultrasonic techniques such as UT-Bscan and Phased Array UT, which were developed during the late '90s, overcame the difficulty in identifying defect orientation. The orientation of crack geometry affects its growth during service. Under torsional loading conditions during service, the crack, in line with the shear stress direction, grows rapidly. The material properties and the crack geometry affect the crack growth rate. The crack close to the outer surface of the shaft would be subjected to high-stress conditions, and the possibility of catastrophic failure is imminent under loading conditions once the crack reaches the outer surface.

The basic parameters of installed hydro plants are the maximum head, turbine power, Generator rotor and shaft, turbine runner, radial bearings at three locations, etc. Estimation of fatigue degradation process involves multi-step processes viz. Crack initiation, growth rate and fracture. The damage tolerance studies of the in-service critical turbine-generator shafts are practised through finite element-based analysis. However, the information on the shaft material, properties, and fracture toughness parameters is not available, particularly for plants in the late 70s. The fatigue crack growth database for the damage tolerance studies is reported for many steel, Aluminium, and stainless steel materials used in the aerospace industry [6], [7]. The severity of the stress at the crack tip is characterized by the elastic stress intensity factor, 'K' [8]. In general, the well-established Paris equation ;

$$\frac{da}{dN} = C(\Delta K)^n \dots\dots\dots(1)$$

where ' $\Delta K$ ' = is the change in stress intensity factor along the crack front ( $\text{MPa}\sqrt{\text{m}}$ );

$da/dN$  = increase in crack length (m/cycle), 'C' & 'n' = constants based on material grade. The constants used for the crack growth used in the previous study were carried out based on the steel grade data of different steels [9]

In this paper, the FEA-based damage Tolerance studies of Turbine and Generator Shaft considering critical cracks identified by UT-Bscan inspection in high-stress regions of the 17.5 MW hydro plant, installed in 1963 and completed service life of more than 60 years, were carried out using Ansys and FRANC3D software. The methodology of estimating the remaining life of a cracked shaft in service through repeat ultrasonic inspection of the shaft at critical crack locations has not been reported in the literature. Estimation of the residual life of the shafts was calculated based on the observed increment in the crack length after a specific period of service and considering other key parameters that have a significant impact on the life, such as changes in vibration amplitudes in the bearing area, magnetic imbalance pull of generator, etc.

## 2.0 NDT INSPECTION OF THE ROTOR SHAFT

The ultrasonic B-Scan mapping was carried out using Modsonic Arjun 30 model equipment, and the observed crack sizes were compared with those of the previous inspection results. The complete shaft surface was covered through the creation of many patches with reference to bolt nos of in the interface flange. Patch length each of 100 mm was made around the circumference and axial direction along the turbine-generator shaft. Also, the probe was set to cover 90 deg segment of the shaft. The pre-NDT measurement patches made on the shaft are shown in Fig. 1. The crack information data has been acquired in all patches. The Turbine Generator shafts have been inspected by Ultrasonic B-scan inspection of the rotor shafts on

critical crack locations identified during the previous inspection program.

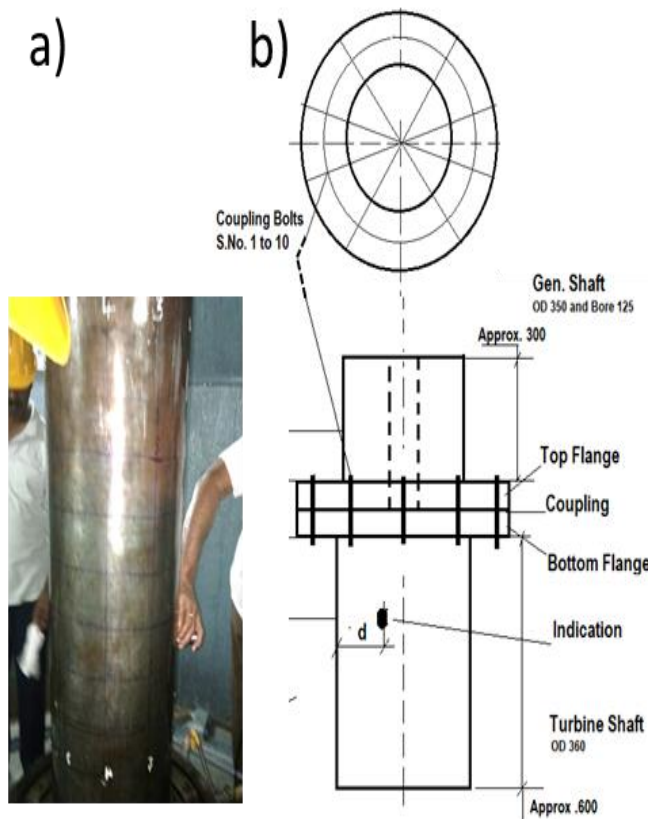


Fig. 1. Patching made on the turbine-generator shaft for UT-Bscan imaging and the locations of bolting joints

The Ultrasonic B-scan imaging was carried out on the 360 mm diameter region of the turbine shaft as well as the accessible region of the Generator bottom end of the shaft above the interface flange as a part of the re-examination of the cracked regions. The change in the size of the crack, if any observed, was carried out during the second inspection cycle. A miniature shear wave probe was used to obtain the cracks located close to the radius region, and the scanning was done in the axial and circumferential directions.

The output spectrum obtained during the UT B-scan imaging is shown in Fig. 2 below. The A-scan spectrum of the critical crack observed is shown in Fig. 3.

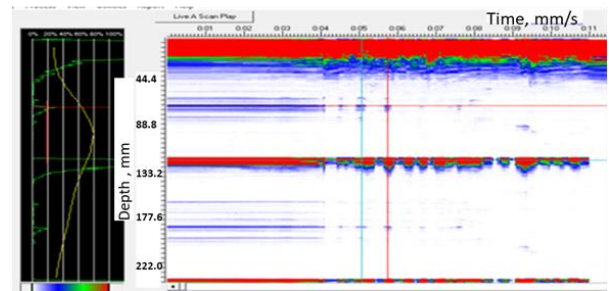


Fig. 2 B-scan imaging results of Crack 7

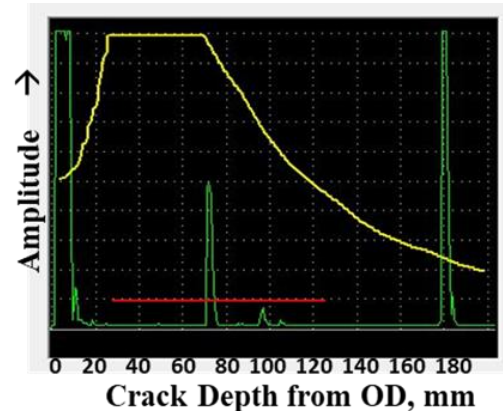


Fig. 3 A-scan results of crack seven at 65.7 mm depth and adjacent minor defects

Other cracks located close to the ID bore region of the turbine shaft were also observed with an Equivalent Reflector Size up to 5.6 mm. The initial NDT inspection showed that the critical crack size was 1.4 mm at a depth of 68 mm from the shaft's OD. The observed crack was 60 mm above the turbine-generator (T-G) interface flange. The number of hours completed service hours after the first inspection was 22760 hrs, equal to 2.6 years. During the second inspection, the size of the crack was observed to be 2.7 mm of equivalent reflector size, and the depth of the crack tip was close to 65.7 mm from the outer surface of the generator shaft in the radial direction. Though the number of years completed after the previous inspection was 4.5 years, the actual number of hours of service indicated by the utility was very low, indicating that the unit was used as a peak loading plant. These cyclic loading conditions invariably cause fatigue damage to the shaft components. The utility reported an increase in vibration amplitude level at the lower guide-bearing region from 110 to 185 microns.

The summary of the details of flaw /defect-like indications observed on the Turbine- Gen. shaft regions is given in Table -1 below

Table 1. Results of ultrasonic A scan data

Crack No.	Defect locations below the T-G interface bolts	Equivalent Reflector Size of defect, (mm)	Depth from the OD surface of the shaft (mm)	Distance From the T-G interface flange (mm)	Remarks
<b>a)</b>	<b>Location: Turbine shaft, Below T-G interface Flange</b>				
1	Between bolts Nos 3 & 4	3.8	97	325	Change in crack size by 0.3 mm
2	10	3.8	171	385	
3	4	<b>5.9</b>	180	585	Near the core region – No change in crack size was observed
4	<b>8</b>	<b>4.6</b>	<b>182</b>	<b>350</b>	
5	9	5.5	185	585	
6	Between bolts Nos 5 & 6	<b>3.8</b>	<b>188</b>	385	Near the core
<b>b)</b>	<b>Location: Generator Shaft, above T-G interface flange</b>				
7	Above the bolt 8	2.7	65.7	60	Increase in crack length by 1.5 mm.
8	Between bolts Nos 5 & 6	2.5	85	105	New Crack observed

### 3.0 FINITE ELEMENT ANALYSIS (FEA) OF THE STRESSES EXPERIENCED BY THE SHAFT

In the present study, the shafts of both the turbine and generator have been considered as an integral part of the rotating system and thus considered as a single body for FEA for simulations. The generator shaft supports the generator's rotor part, which comprises the electric poles and spider assembly. Since the system is of vertical type, the combined weight of the shaft is considered to act in the direction of vertical gravity. The view of the 3D model of the geometry of the turbine-generator rotor shaft of 17.5 MW studied is shown in Fig. 4. The radius of the generator rotating mass component was 3158 mm, depicting the rotor poles attached to the shaft through the spider web assembly.

The details of the turbine-generator shaft per the design conditions are as follows.

- Turbine type : Francis, Vertical
- Mass of turbine shaft : 2.4686 tons

- Mass of Generator shaft : 5.652 tons
- Gen. poles & spider assembly : 47.04 tons
- Mass of turbine runner : 4.3 tons
- RPM of the Generator : 600 rpm

The Finite Element Analysis using Ansys 19.1 software in combination with the Crack growth rate in the shaft was carried out using FRANC3D modules. The complete assembly of the generator & turbine shaft has been modelled using the design modeller as per the design. The 3D CAD model geometry of the Turbine and generator shaft assembly was made using Ansys software 19.1 and meshed with Hexa-tetrahedral elements in ANSYS software. A fine tetrahedral element mesh was used to accurately predict the shaft's stress. The total number of elements in the discretized model was 1648422. The rotor poles are attached to the shaft through the spider web assembly. The weight of the generator rotating mass (rotor) disc comprising all the poles, spider assembly, and turbine assembly components, viz. blades, were considered. The 3D



model of the Turbine-generator assembly and the discretized model are shown in Fig. 4.

A total of ten poles were connected to the generator shaft through the spider assembly as solid shaft attachments. Accordingly, the pole masses were solid bodies attached to the shaft. The mass of the poles and other masses are modelled as a solid disc and attached to the shaft. The bearing support regions at three locations along the shaft are considered for displacement. The mass of the turbine runner was attached to the shaft as a point mass. The rotor attached to the shaft was modelled as a solid cylinder with the same mass as that of the actual rotor.

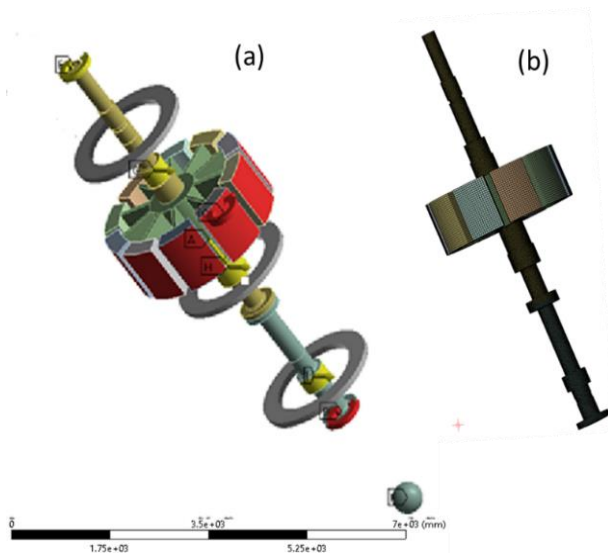


FIG. 4 3D geometry of Turbine-Generator shaft with bearing support (a) and discretized geometry (b)

To account for various loss components, the shaft structural analysis considered 20% more torque, corresponding to the uprated generation capacity of 17.5 MW. The loss components considered in the present study include unbalanced magnetic pull (3%), turbine efficiency loss (15%) and generator efficiency loss of 2%. Thus the total torque load considered for the analysis is 21 MW, which is equal to  $334 \times 10^6$  Nmm. The mass of the turbine rotor was considered as a lumped mass attached to the turbine bottom flange. The earth's gravitational acceleration was applied to the complete assembly to bring the effects of the self-weight of the assembly and the turbine mass.

The rotor's mass, the shaft's self-weight and the turbine's mass are considered for the analysis. Considering the

efficiency of the turbine and generator, misalignment, magnetic imbalance, etc., the equivalent von Mises stress and the shear stress experienced during the running of the Turbine were estimated by static structural analysis. The boundary conditions used for the analysis are ;

- Torque proportional to 21 MW on the turbine-generator shaft in line with the rotational direction
- While the torque was applied in the opposite direction at the generator pole ends, proportional to the turbine torque, The displacement at three bearing locations of 350 microns
- Imbalance in the rotor was considered through the addition of 10kg mass to a pole. At the same time, 10kg mass was reduced in the pole opposite to the added mass pole. This facilitates the constant mass of poles with imbalance.

For crack growth rate estimation, the following analysis was carried out on the meshed model of the shaft.

- During the turbine operation, the torque exerted onto the turbine runner by the high-pressure stream is considered consumed by the generator rotor in terms of proportional electrical loading.
- The translation displacements were considered at three bearing regions of the shaft.
- Estimation of stress levels of the shaft under defect-free conditions for uprated capacity conditions to identify critical stress regions
- Estimation of the crack growth for each crack length step of 0.35mm was followed during fatigue cycling, and the number of cycles completed for each step was obtained using the FRANC3D™ program.
- The residual life of the shaft was calculated by extrapolating the crack growth rate results.

## 4.0 RESULTS AND DISCUSSION

### 4.1 Stress analysis of the turbine-generator integrated shaft

Since the torsional stress value close to the shaft's OD surface is maximum compared to the central region, a crack close to the OD surface has been considered for the analysis.

The rotational speed of 600 rpm of the generator shaft with the global Y axis as the rotational axis was considered in the FEA maximum. The magnitude of the equivalent von Mises stress in the generator shaft varies close to the ID side bore and is observed to be 146.4 to 170.3 MPa, while the shear stresses reach up to 94.6 MPa as shown in Fig. 5 & 6. The allowable maximum tensile stress of the shaft material was 540 MPa. The von Mises stress in the turbine shaft reaches a maximum value of 129.1 MPa near the root radius region of the shaft interface flange. The shear stress observed was 64.7 to 74.5 MPa on the turbine shaft.

The maximum stress location is observed in The root radius region of the bottom flange of the generator shaft, which has shown the highest stress levels. The observed critical crack was in that region and thus affected the life

of the shaft. Since the complete torque is taken out in the pole area, the regions above the pole area have shown very low levels of stress. The average stress at the smallest cross-section of the shaft is 21.3 MPa, which is much less than the yield strength of the forged steel grade ess of the shaft material ( 275 MPa ). These stress values were very much within the minimum yield strength of the forged shaft material assumed (275 MPa). However, the elemental average von Mises stress values in the Generator and turbine shaft were much less (42 to 48 MPa ), while the shear stress values were 23.2 to 27 MPa. From the viewpoint of design specifications as per ASME B106.1, the shear stress of up to 40% of allowable yield stress in tension is considered acceptable, which is calculated to be approx. 110 MPa.[10]

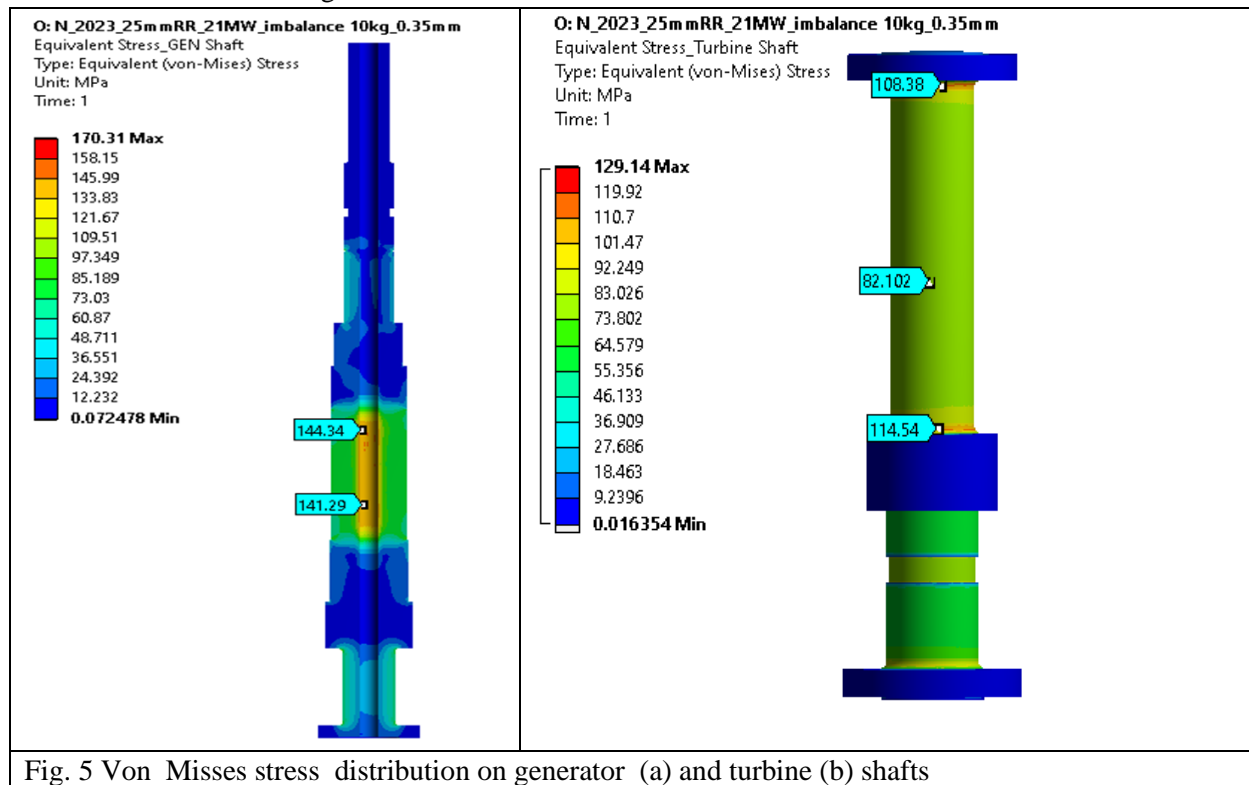


Fig. 5 Von Mises stress distribution on generator (a) and turbine (b) shafts

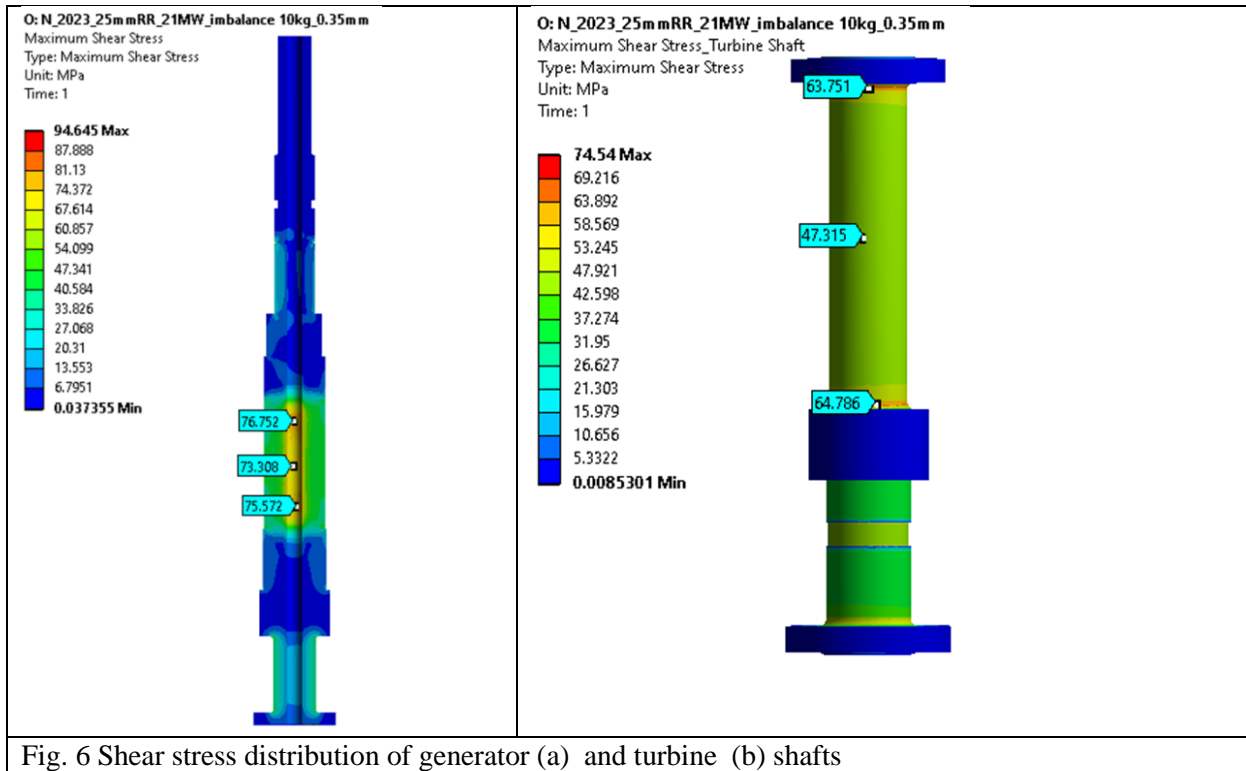


Fig. 6 Shear stress distribution of generator (a) and turbine (b) shafts

## 4.2 Fatigue crack growth analysis

In hydro turbines, the torsional shear stresses are maximum at the OD surface of the shaft. Generally, cracks opened to the surface (surface cracks) are not permissible for critical Turbine and generator shafts. Thus, the observed crack at minimum depth from the OD of the shaft has been considered for the crack growth study as this gives the lowest residual service life. The reported literature on the combined mixed mode I + III fatigue crack growth of steel materials using compact test specimens with cracks oriented at  $45^\circ$  angles has shown a higher growth rate. Vaziri and Nayeb-Hashemi, 2005 have studied the effect of Mode III crack surface interaction in circular shafts on the stress intensity and reported that the Mode III crack growth follows Paris law when effective stress is considered in the crack driving force. The turbine-generator shafts of Hydro plants operating at lower speeds with high rotating masses experience maximum stress intensities in the Mode-III stress intensity factor [11]. In the present study, the crack growth analysis was done under mixed mode  $K_{\text{equivalent}}$  condition. This accounts for all three types of stress conditions at the crack tip field condition as given by ;

$$K_{\text{equivalent}} = \sqrt{(K_I^2 + \gamma_{II} K_{II}^2 + \gamma_{III} K_{III}^2)}$$

Where

$K_I$  = Tensile stress mode

$K_{II}$  = Shear stress parallel to the crack plane

$K_{III}$  = shear stress parallel to the crack front

$\gamma_{II}$  and  $\gamma_{III}$  are constants, assumed as =1

The Gamma represents the relative contributions of Mode I and Mode II fracture modes and it requires exhaustive laboratory Experiments. In the present case, the values of  $\gamma_{II}$  and  $\gamma_{III}$  are assumed to be equal to 1.

The steps followed during the crack growth study include;

- A local sub-model, considering the small area at the top and bottom of the cracked region, was created
- The crack growth analysis of the inserted cracks in the sub-model is considered to assess the stress intensity during fatigue loading conditions, considering the load spectra from the static analysis. Based on the crack tip stress intensities at the crack tip area, the growth of the crack takes place in a preferential direction. The number of fatigue cycles (dN) completed corresponding to incremental crack

length (dA) was estimated for each growth step. The flow diagram showing the various steps followed in the life estimation of the cracked shaft is shown in Fig. 7.

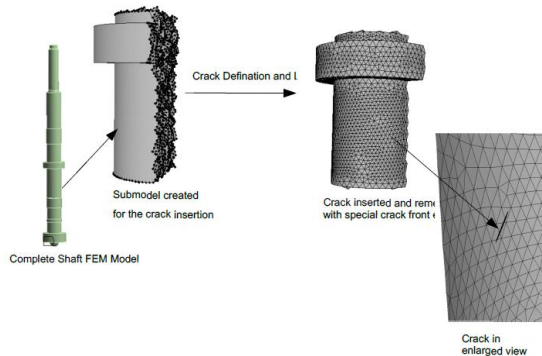
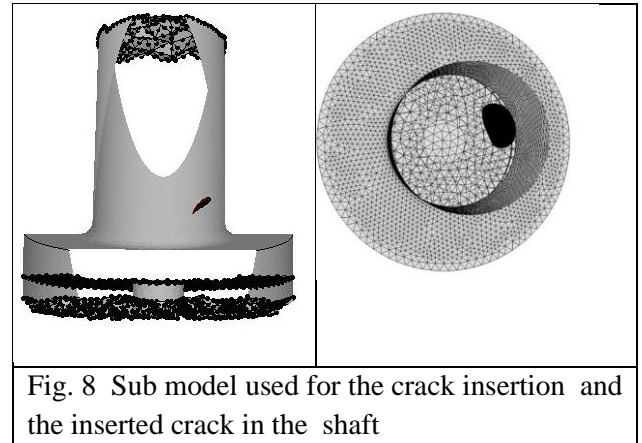


Fig. 7 Steps followed in crack growth analysis

As there was no data on the generator shaft's material grade, high-carbon steel with forged conditions was assumed. The multiple variables for the Paris constant and exponents were considered, along with material properties, as given below.

Young's modulus : 200 GPa  
Poisson's ratio : 0.3  
Yield strength : 275 MPa  
Tensile strength : 540 – 640 MPa  
Fracture toughness : 85 MPa  $\sqrt{m}$   
Paris constant, C : 1E-11 & 1E-12 m/cycle  
Paris exponent (n) : 2.0 to 2.85

The incremental growth of the crack was carried out in different steps. After each growth step, the modified crack dimension was automatically inserted into the shaft. The subsequent crack growth cycle is continued with new stress intensity factors at the crack tip. The inserted crack geometry, along with crack front growth cycles, are shown in Fig. 8. The growth of the crack was estimated for multiple fatigue cycles up to twenty steps. The data on crack length with respect to each fatigue cycle were extrapolated so as to obtain the number of cycles required for the crack to reach the surface of the shaft, which is considered as the end of life.



The result of the rate of growth under different fracture mechanic parameter conditions is given in Table 2. The result of the calculated stress intensity factor along the crack front for the crack step 20 clearly indicated the role of all three modes of stress conditions viz. KI, KII and KIII are linked to crack growth. The maximum stress intensity value at the crack front for the KIII mode is much higher than for the KI mode, as shown in Fig. 9.

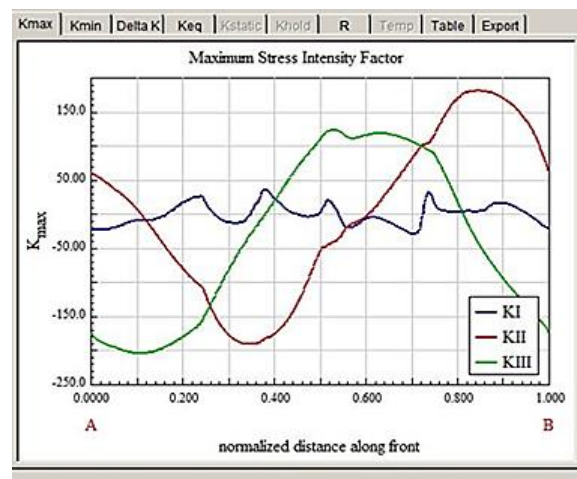


Fig. 9 Maximum stress intensity factor observed in different modes of crack growth

Thus, the prediction of residual life was carried out using K equivalent mode for the analysis. The verification of optimum conditions for the fatigue crack growth rate analysis includes the following key points pertaining to crack information such as ;

- Actual no. of hours completed
- Change in crack length observed
- Imbalance and offset conditions linked to vibration
- Stress conditions based on the efficiency factors



Based on the initial data, the suitability of the fracture mechanic parameters such as "C" and "n" aligning with the actual no. of fatigue cycles and crack length were considered. The threshold stress intensity factor considered for the material is  $5\text{MPa}\sqrt{\text{m}}$ . The observed SIF was higher than the  $K_{th}$  value set in the analysis. After each step, the stress corresponding to the modified dimension of the crack was considered, and the growth cycle of the crack was continued. The fatigue crack growth was studied for 20 growth steps, with an increase in the crack length parameter of 0.3 mm. Extrapolation of the crack growth rate data was followed after the complete cycles and the cycles corresponding to crack length reaching the OD surface of the shaft. The predicted life of the shaft as per the previous crack growth study was 3.35 years without considering the magnetic imbalance, displacement conditions and varied Paris parameters.

The crack growth linked to the service hours of operation was re-estimated with modified constants of "C" and "n." The results are given in Table 2.

The calculated number of cycles based on the actual number of hours completed in service equals  $8.199 \times 10^8$ . The results indicated that the growth of crack length of 2.6625 mm requires  $8.018 \times 10^8$  cycles from the previous crack length of 1.3mm. Under severity conditions of imbalance, displacement in the bearing linked to an increase in the magnitude of vibration, the number of cycles was matched with that of the completed service hours equal to  $8.199 \times 10^8$  cycles, which closely matches with that of incremental growth of 2.6625 mm under parameters of  $n=2.85$  and  $C=1 \times 10^{-12}$ . The predicted growth

Table 2: Results of Crack growth rate of 65.7mm depth crack under different Paris constant and exponent values

Growth steps	Crack length, mm	$n = 2$ $C = 1 \times 10^{-11}$	$n = 2.5$ $C = 1 \times 10^{-11}$	$n = 2.85$ $C = 1 \times 10^{-12}$
1	1.34	$2.87 \times 10^7$	$2.67 \times 10^7$	$2.54 \times 10^8$
2	1.68	$5.18 \times 10^7$	$4.71 \times 10^7$	$4.42 \times 10^8$

3	2.01	$7.9 \times 10^7$	$6.33 \times 10^7$	$5.85 \times 10^8$
4	2.32	$8.75 \times 10^7$	$7.68 \times 10^7$	$7.03 \times 10^8$
5	2.66	$1.2 \times 10^8$	$8.85 \times 10^7$	$8.18 \times 10^8$
6	2.96	$1.15 \times 10^8$	$9.86 \times 10^7$	$8.86 \times 10^8$
7	3.28	$1.27 \times 10^8$	$1.74 \times 10^8$	$9.58 \times 10^8$
8	3.60	$1.38 \times 10^8$	$1.15 \times 10^8$	$1.02 \times 10^9$
9	3.90	$1.48 \times 10^8$	$1.22 \times 10^8$	$1.08 \times 10^9$
10	4.20	$1.57 \times 10^8$	$1.29 \times 10^8$	$1.13 \times 10^9$
11	4.51	$1.66 \times 10^8$	$1.35 \times 10^8$	$1.18 \times 10^9$
12	4.81	$1.74 \times 10^8$	$1.40 \times 10^8$	$1.22 \times 10^9$
13	5.17	$1.81 \times 10^8$	$1.45 \times 10^8$	$1.25 \times 10^9$
14	5.45	$1.89 \times 10^8$	$1.50 \times 10^8$	$1.29 \times 10^9$
15	5.74	$1.95 \times 10^8$	$1.55 \times 10^8$	$1.32 \times 10^9$
16	6.03	$2.02 \times 10^8$	$1.59 \times 10^8$	$1.35 \times 10^9$
17	6.34	$2.08 \times 10^8$	$1.62 \times 10^8$	$1.38 \times 10^9$
18	6.63	$2.14 \times 10^8$	$1.66 \times 10^8$	$1.41 \times 10^9$
19	6.90	$2.19 \times 10^8$	$1.69 \times 10^8$	$1.43 \times 10^9$
20	7.17	$2.25 \times 10^8$	$1.73 \times 10^8$	$1.45 \times 10^9$

cycle based on the fit corresponding to the crack length of 2.7 mm is  $7.96 \times 10^8$  cycles, and the predicted cycle variation was marginally close to 2.97%. The extrapolations were based on the logarithmic fit with  $R^2$  value of more than 0.99. Fig. 10 & 11 show the extrapolated curve fit data of growth cycles with respect to crack lengths in different growth steps and the incremental crack length with ref. to the radial direction towards the OD of the shaft.

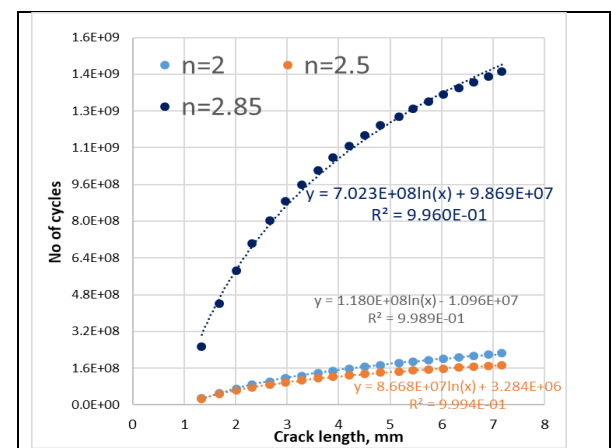


Fig. 10. Curve fit of crack length growth cycle with respect to the crack length

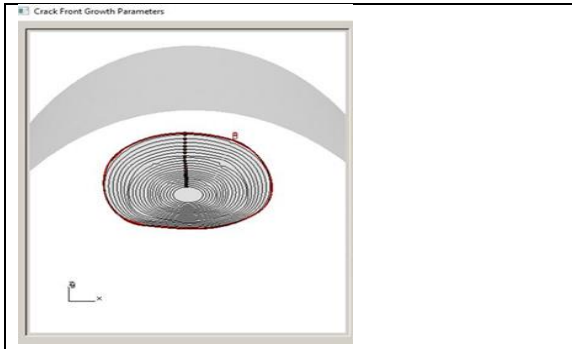


Fig 11 Incremental step result of Crack size towards OD

The calculated number of cycles required for the crack to reach 65.7 mm onto the shaft's OD surface was  $3.03\text{E}+09$  cycles, and the corresponding estimated residual service life of the shaft amounts to 9.16 years.

## 5.0 CONCLUSIONS

The pragmatic approach for the residual life estimation of the cracked turbine generator shafts indicated the need for the selection of appropriate fracture mechanics parameters through the repeat inspection cycles of the observed crack length linked to the expended service life along with displacement linked to vibration, imbalances etc., for precise prediction of the residual life of the shaft components. Thus, the hypothesis of prediction of the residual life of cracked shafts would be based on the materials' Paris constants being accurately determined and that the crack length is precisely known as these parameters are crucial in calculating the residual life of a component.

## 6.0 ACKNOWLEDGEMENTS

The author thanks the management of Central Power Research Institute (CPRI), Bangalore, India, for supporting the new methodology adopted in the niche area and permitting the author to publish this paper.

## 7.0 REFERENCES

- [1] O. P. Rahi and A. K. Chandel, "Refurbishment and uprating of hydropower plants - A literature review," *Renew. Sustain. Energy Rev.*, vol. 48, no. 2015, pp. 726–737, 2015, doi: 10.1016/j.rser.2015.04.033.
- [2] M. M. Lima, C. Godoy, P. J. Modenesi, J. C. Avelar-batista, A. Davison, and A. Matthews, "Coating fracture toughness determined by Vickers indentation : an important parameter in cavitation erosion resistance of WC – Co thermally sprayed coatings," vol. 178, pp. 489–496, 2004, doi: 10.1016/S0257-8972.
- [3] X. Liu, Y. Luo, and Z. Wang, "A review on fatigue damage mechanism in hydro turbines," *Renew. Sustain. Energy Rev.*, vol. 54, pp. 1–14, 2016, doi: 10.1016/j.rser.2015.09.025.
- [4] J. Hou, R. Wescott, and M. Attia, "Prediction of fatigue crack propagation lives of turbine discs with forging-induced initial cracks," *Eng. Fract. Mech.*, vol. 131, pp. 406–418, 2014, doi: 10.1016/j.engfracmech.2014.08.015.
- [5] P. E. Bold, M. W. Brown, and R. J. Allen, "A Review of Fatigue Crack Growth in Steels Under Mixed Mode I and II Loading," *Fatigue Fract. Eng. Mater. Struct.*, vol. 15, no. 10, pp. 965–977, 1992, doi: 10.1111/j.1460-2695.1992.tb00025.x.
- [6] R. G. Forman, V. Shivakumar, J. W. Cardinal, L. C. Williams, and P. C. McKeighan, "Fatigue crack growth database for damage tolerance analysis," *Natl. Tech. Inf. Serv.*, vol. 15, no. August, pp. 1–126, 2005.
- [7] W. O. Clark, "Fatigue crack growth characteristics of rotor steels," *Eng. Fract. Mech.*, vol. 2, no. 4, 1971, doi: 10.1016/0013-7944(71)90015-4.
- [8] P. C. Paris, "Fracture mechanics and fatigue: A historical perspective," *Fatigue Fract. Eng. Mater. Struct.*, vol. 21, no. 5, pp. 535–540, 1998, doi: 10.1046/j.1460-2695.1998.00054.x.
- [9] S. Seetharamu, T. Jagadish, and R. R. Malagi, *Fatigue , Durability , and Fracture Mechanics*. 2019.
- [10] ANSI/ASME, *ANSI-ASME-B106-1-1985.pdf*, vol. 2. 1985.
- [11] A. Vaziri and H. Nayeb-Hashemi, "The effect of crack surface interaction on the stress intensity factor in Mode III crack growth in round shafts," *Eng. Fract. Mech.*, vol. 72, no. 4, pp. 617–629, 2005, doi: 10.1016/j.engfracmech.2004.03.014.